European Journal of Medicinal Chemistry Reports 7 (2023) 100099

HOSTED BY

Contents lists available at ScienceDirect

European Journal of Medicinal Chemistry Reports

journal homepage: www.editorialmanager.com/ejmcr/default.aspx

Non-cytotoxic aza-BODIPY triterpene conjugates to target the endoplasmic reticulum

Sophie Hoenke, Benjamin Brandes, René Csuk *

Martin-Luther University Halle-Wittenberg, Organic Chemistry, Kurt-Mothes-Str. 2, D-06120, Halle (Saale), Germany

ARTICLE INFO

Keywords:
Triterpenes
aza BODIPY
Endoplasmic reticulum
Malignant cells

ABSTRACT

In search of suitable tool to target the endoplasmic reticulum of human tumor cells, a non-cytotoxic aza-BODIPY derivative was designed and accessed in a simple synthesis in a few steps from commercially available starting materials. This aza-BODIPY was conjugated to 3-*O*-acetyl-triterpene carboxylic acids (glycyrrhetinic, ursolic, oleanolic, and betulinic acid) using a piperazinyl spacer. The resulting conjugates exhibited no cytotoxicity but were able to selectively target the ER.

1. Introduction

Visualization of the structures of (living) cells is most important to understand metabolic processes in detail. Thereby, the endoplasmic reticulum (ER) plays a major role in the survival of mammalian cells but also in their maintenance and homeostasis. Since in ER vital processes such as protein assembling, protein folding and post-translational modifications take place, investigations concerning the ER have gained increased attention. ER stress is known to lead to dysregulation. This dysregulation is considered to play an important role in non-communicative diseases such as diabetes and cancer but also in neurodegenerative diseases and strokes [1].

Visualization of organelles and their cellular processes can be done most preferentially by fluorescence microscopy, and small fluorescent molecules are often used to fluorescently label the organelles [2]. One of the prerequisites for successful investigations is a superior target selectivity of these molecular probes. Several BODIPYs such as ER-Tracker ™ Green and ER-Tracker ™ red (Fig. 1), both holding a glibenclamide moiety, are most often used; they are commercially available [1]. Several BODIPY-conjugates targeting different organelles or metabolic processes have been reported recently, among them conjugates with platinum drugs [3–11] or curcumin [12], paclitaxel [13–15], PEG conjugates [16–18], chlorambucil [19], capsaicin [20], isoxazoles [21], and mertansine [22]. All of these were intended to act as cytotoxic agents. One of the major aims of this study was to develop a molecular fluorescent probe-based bio-imaging and bio-sensing tool for non-invasive monitoring of biological processes in real time to provide dynamic information about for biological analysis. This has been accomplished by nanodots [23] as well as by fluorescence probes [24–28].

Recently, two studies dealt with BODIPY-triterpene conjugates [29, 30]. These compounds were also of moderate cytotoxicity but held improved tumor cell selectivity as compared to other conjugates. Furthermore, it was shown that triterpenoic acid amides holding a distal rhodamine (B or 101) unit are of superior cytotoxicity thereby acting as a mitocanic agent [31] while triterpene-safirinium conjugates [32] target the ER. Their cytotoxicity was significantly diminished as compared to the rhodamine conjugates [25]. BODYPY FL labelled triterpenoids were shown to hold good cytotoxicity for MCF-7 human breast adenocarcinoma cells but not to other cell lines [30]. From these observations and keeping in mind that the cytotoxicity of triterpene amide conjugates is strongly governed by the distal substituent we assumed that triterpene aza-BODIPY conjugates might be of low cytotoxicity but should provide a good selectivity for the ER.

Our previous studies also showed that the “linker” between the fluorophore and the triterpenoic skeleton should be a piperazinyl moiety [31]. Hence, we set out to access these compounds by synthesizing a piperazinyl substituted BODIPY first followed by coupling this molecule to 3-*O*-acetyl substituted triterpenoic acids [30], such as glycyrrhetinic acid (**GA**), ursolic (**UA**), oleanolic acid (**OA**) and betulinic acid (**BA**).

2. Results and discussion

The synthesis (Scheme 1) of the BODIPYs started from commercially available 4-hydroxy-acetophenone (**1**) whose aldol condensation with benzaldehyde gave 93% of (*E*)-configurated chalcone **2** [30]. The configuration of the double bond was determined from the magnitude of

* Corresponding author.
E-mail address: rene.csuk@chemie.uni-halle.de (R. Csuk).

https://doi.org/10.1016/j.ejmcr.2022.100099
Received 27 October 2022; Received in revised form 13 December 2022; Accepted 25 December 2022
Available online 27 December 2022

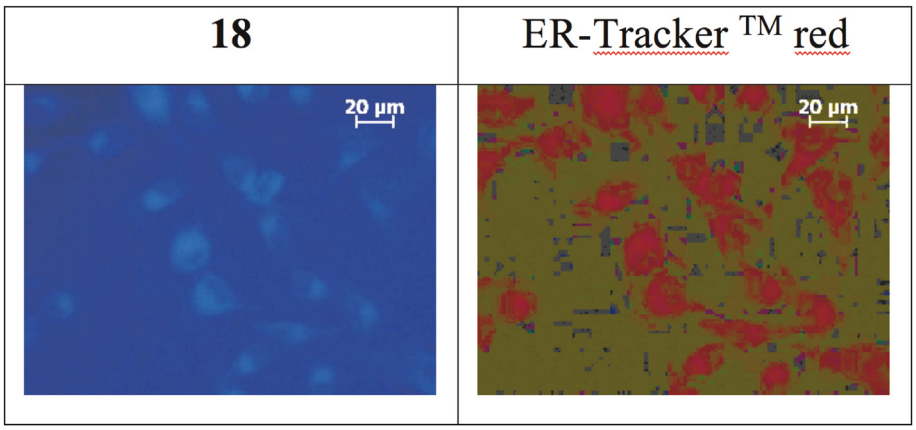

Fig. 1. Extended investigation of **18** and A375 cells: Fluorescence microscopic images (scale bar 20 µm), and ER-Tracker ™ red (staining of the endoplasmic reticulum); double staining experiment. (For interpretation of the references to color in this figure legend, the reader is referred to the Web version of this article.)

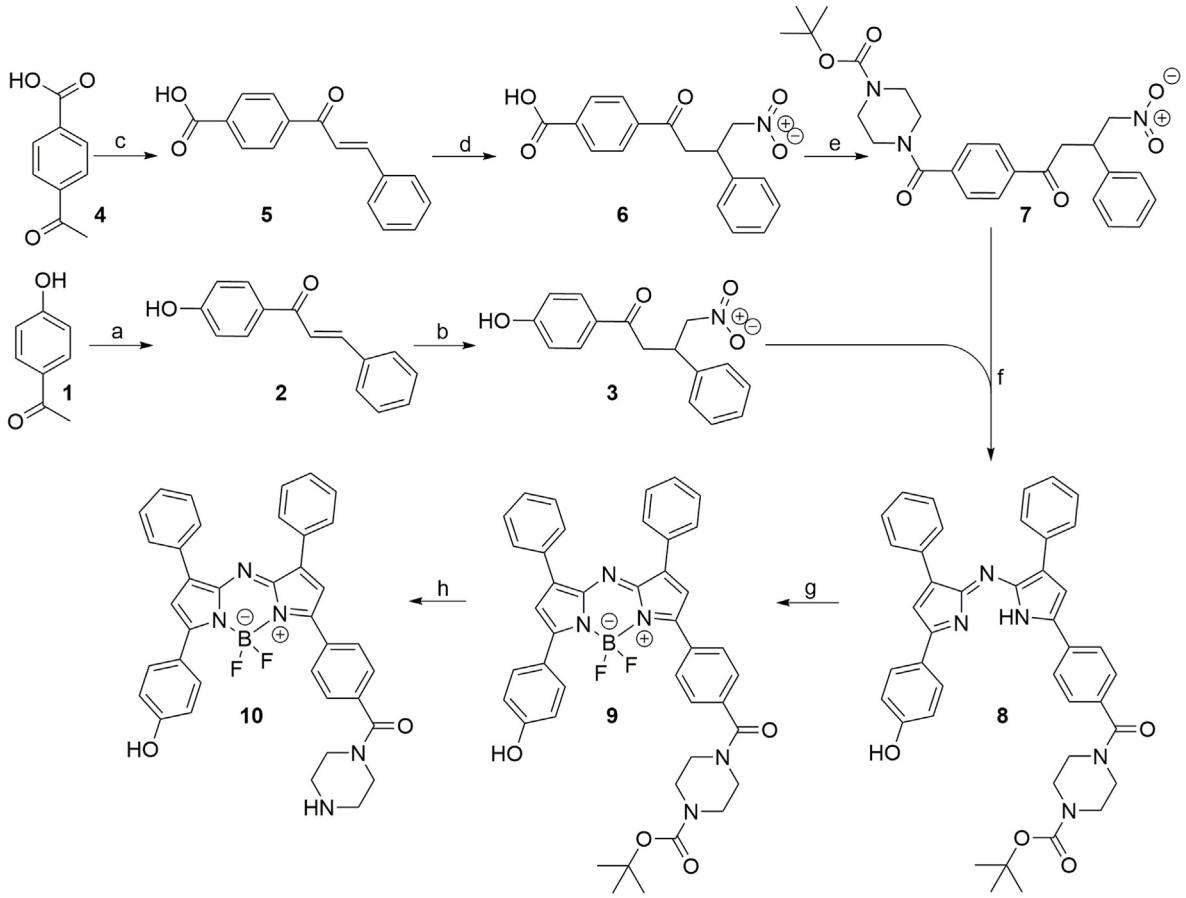

Scheme 1. Synthesis of aza-BODIPY (**10**); a) NaOH, EtOH, H_2O, room temperature, 30 min → benzaldehyde, room temperature, 93%; b) CH_3NO_2, KOH, MeOH, room temperature → reflux, 6 h, 64%; c) KOH, H_2O, EtOH, room temperature → benzaldehyde, room temperature, overnight., 90%; d) CH_3NO_2, KOH, MeOH, room temperature → reflux, 6 h, 98%; e) cat. DMF, oxalyl chloride, DCM, 0 °C → room temperature, 1.5 h → TEA, Boc-piperazine, 2 h, room temperature, 72%; f) $NH_4CH_3CO_2$, n-BuOH, reflux, 8 h, 54%; g) $BF_3{\cdot}Et_2O$, DIPEA, room temperature, overnight, 20%; h) HCl in 1,4-dioxane, MeOH, room temperature, 91%.

the ^3J coupling constant of the olefinic hydrogen substituents of 15.5 Hz being typical for an (*E*) configuration. Reaction of **2** with nitromethane furnished **3** [34] in 64% isolated yield. The presence of a nitro substituent in **3** and **6** [29] (vide infra) is characterized by the presence of characteristic signals in their IR spectra at $\tilde{\nu} = 1554$ and 1375 cm^{-1} (for **3**) and $\tilde{\nu} = 1549$ and 1378 cm^{-1} (for **6**). In this divergent approach, 4-acetyl-benzoic acid (**4**) was coupled with benzaldehyde to furnish **5** [35,36] whose reaction with nitromethane yielded **6**. Reaction of **6** with oxalyl chloride in the presence of DMF (cat.) followed by the reaction with Boc-piperazine furnished **7** in 72% yield. Coupling of **3** and **7** in refluxing *n*-BuOH in the presence of ammonium acetate gave **8** whose cyclisation to BODIPY **9** was accomplished with boron trifluoride diethyl etherate and diisopropylethylamine (DIPEA) overnight. Deprotection of **9** gave BODIPY **10** in 91% yield. This compound is characterized in its ^{19}F NMR by a signal multiplet at $\delta = -130.85$ to -132.06 ppm; in the ^{11}B NMR spectrum a signal at $\delta = 1.01$ ppm as a virt. triplet holding a $J_{B,F} = 31.6$

Hz is found; the chemical shift and the magnitude of the coupling constant is typical for this type of compounds [37].

The triterpenoic acids **GA**, **UA**, **OA** and **BA** (Scheme 2) were acetylated as previously described [24] resulting in well-known acetates **11**–**14**. Reaction of the acetates with oxalyl chloride/DMF (cat) followed by adding BODIPY **10** furnished the conjugates **15**–**18** in 47–70% isolated yields (Scheme 3). As exemplified for oleanolic acid derived **17**, the conjugate showed a ^{11}B NMR chemical shift of $\delta = 0.97$ ppm (t, $J = 31.4$ Hz) and a ^{19}F NMR $\delta = -129.19$ to -133.50 ppm, together with the typical signals of the triterpenoid skeleton and the piperazinyl residue hence proving the structure of the conjugate.

To assess the cytotoxicity of the compounds, SRB assays were performed employing several human tumor cell lines, such as A375 (melanoma), HT29 (colon adenocarcinoma), MCF7 (breast adenocarcinoma), A2780 (ovarian carcinoma), HeLa (cervical adenocarcinoma) as well as non-malignant cell lines NIH 3T3 (murine fibroblasts) and HEK293 (human embryonic kidney). The results from these assays are summarized in Table 1. Most of the precursors of the final compounds **15**–**18** were found to be not cytotoxic at all (cut-off of the assay 30 μM). Compounds **2** and **5** held some cytotoxicity for all cell lines. This is in excellent agreement with previously reported data on the cytotoxicity of chalcones [38–41]. Thereby, the presence of an α,β-unsaturated ketone seems crucial for the cytotoxic activity since neither **3**, **6** nor **7** showed a cytotoxic effect to the cells. Piperazinyl-substituted **10** was cytotoxic for all cell lines but without any selectivity.

Upon coupling with the acetylated triterpenoic acids **11**–**14**, **10** lost all cytotoxicity; consequently, target compounds **15**–**18** were not cytotoxic at all within the cut-off of the assay (30 μM). This represents a significant improvement in properties compared to BODIPY FL substituted triterpenes, as the latter compounds held some residual cytotoxicity for some cell lines thus limiting their application in living systems [30].

Fluorescence microscopy allowed to determine the localization of the compounds as exemplified for **18**. Visual inspection of the cells showed compound **18** not to be in the nucleus of the cells while double staining of the cells with **18** and rhodamine 123 excluded its localization in the mitochondria. Staining with ER tracker ™ red, however, revealed that **18** ends up in the ER of the cells (Fig. 1).

It cannot ruled out, however, that the probe affects the biological activity of the cells inasmuch as it is known that even unsubstituted ursolic acid participates in metabolic re-wiring and epigenetic re-programming in human prostate cancer [42]. However, no significant changes in the morphology of the cells have been observed upon incubation for 2 days. Triterpenes, as exemplified for asiatic acid, might enter the endoplasmic reticulum, too, but this process triggered in PPC-1 prostate cancer cells a rapid caspase-dependent cell death within several hours of treatment [43]. Furthermore, it cannot completely excluded that triterpenoic probes might exert an indirect effect onto the cell metabolism by binding on chaperones as previously exemplified for triterpenoid celastrol [44]. Additional experiments showed that also **8** is able to enter the cells and to accumulate in the ER; as previously reported, the same holds true for several safirinium triterpene conjugates [32]. However, no significant changes in the morphology of the cells were observed.

3. Conclusion

The labeling and bio-visualization of living cells has come into the focus of scientific interest, and many theranostic drugs have been developed so far. In search of a suitable tool to target the endoplasmic reticulum (ER) of human tumor cells, we designed a non-cytotoxic aza-BODIPY **10** that was accessed in a simple synthesis in few steps from commercially available starting materials. This aza-BODIPY was conjugated to 3-*O*-acetyl-triterpene carboxylic acids (glycyrrhetinic, ursolic, oleanolic, and betulinic acid) using a piperazinyl spacer between the triterpenoid skeleton and the aza-BODIPY scaffold. The resulting conjugates exhibited no cytotoxicity (as shown by SRB assays using a cut-off of 30 μM) but they were able to selectively target the ER (as shown by fluorescence microscopy and staining experiments). Due to the absence of any cytotoxic effects, these novel triterpene aza-BODIPY conjugates are equally suitable for the investigation of cancer cells as well as of non-malignant cells.

4. Experimental part

4.1. General

4-Hydroxyacetophenone (**1**) and 4-acetyl-benzoic acid (**4**) were obtained from local suppliers; Ursolic, betulinic and oleanolic acid were obtained from Betulinines (Stribrna Skalice, Czech Republic) and glycyrrhetinic acid was bought from Orgentis GmbH (Neugatersleben, Germany) and used as received. Equipment was used as previously described [24].

4.2. Cell lines and culture conditions

The biological studies were performed employing the human cancer cell lines A375 (malignant melanoma), HT29 (colon adenocarcinoma),

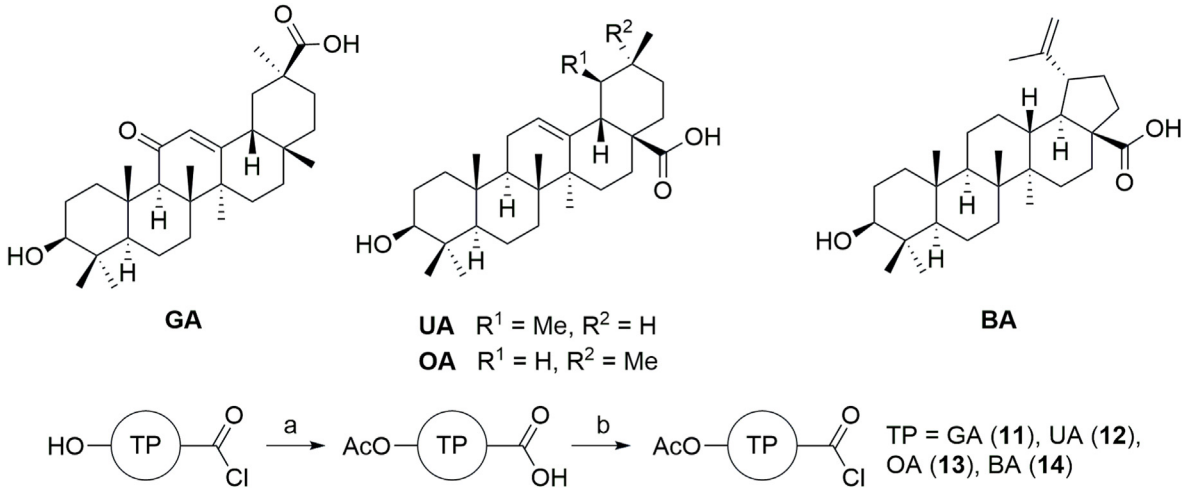

Scheme 2. Structure of parent triterpenoic acids **GA**, **UA**, **OA** and **BA**, their conversion into 3-*O*-acetates and their activation yielding the corresponding acid chlorides.

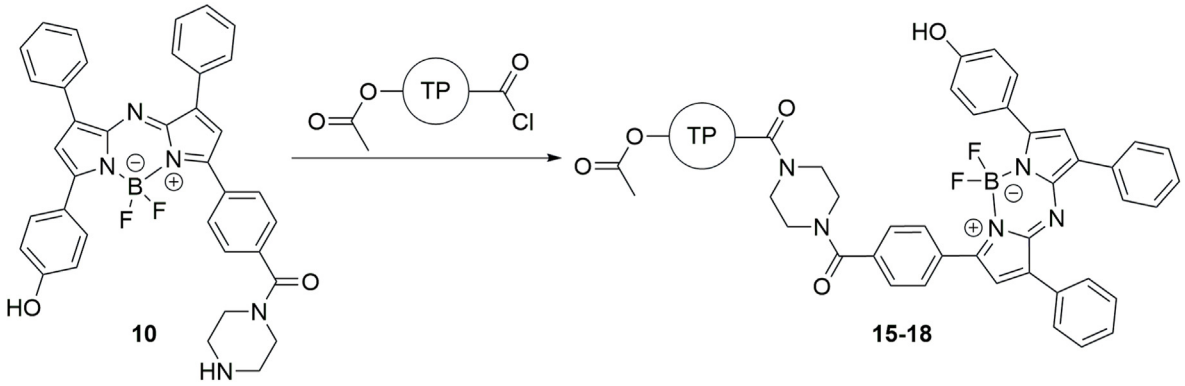

Scheme 3. Synthesis of aza-BODIPY conjugates **15**–**18**: TEA, DCM, room temperature, overnight; yields: **15** (70%), **16** (63%), **17** (47%), **18** (50%).

Table 1
Cytotoxicity of compounds: starting materials **2**, **3**, **5**–**8**, aza-BODIPY derivatives **9** and **10** and corresponding triterpenoid derivatives **15**–**18** (EC_{50}-values in μM from SRB-assays) after 72 h of treatment; the values are averaged from three independent experiments performed each in triplicate, confidence interval CI = 95%; mean ± standard mean error; malignant cell lines: A375 (melanoma), HT29 (colon adenocarcinoma), MCF-7 (breast adenocarcinoma), A2780 (ovarian carcinoma), HeLa (cervical adenocarcinoma); non-malignant: NIH 3T3 (murine fibroblast), HEK293 (human embryonic kidney) were tested.

	A375	HT29	MCF7	A2780	HeLa	NIH 3T3	HEK293
2	5.44 ± 0.3	9.06 ± 0.8	7.61 ± 0.8	9.53 ± 0.9	8.38 ± 0.2	21.4 ± 2.1	7.66 ± 0.1
3	>30	>30	>30	>30	>30	>30	>30
5	14.4 ± 1.0	20.92 ± 0.6	13.8 ± 1.2	19.1 ± 2.0	21.4 ± 1.2	>30	17.03 ± 0.7
6–**9**	>30	>30	>30	>30	>30	>30	>30
10	7.22 ± 0.4	6.19 ± 0.3	6.88 ± 0.8	10.56 ± 0.7	6.23 ± 0.3	6.38 ± 0.9	10.59 ± 0.3
15–**18**	>30	>30	>30	>30	>30	>30	>30

MCF-7 (breast cancer), A2780 (ovarian carcinoma), non-malignant murine fibroblasts NIH 3T3 and non-malignant human embryonic kidney cells (HEK293). All cell lines were obtained from the Department of Oncology (Martin-Luther-University Halle Wittenberg). Cultures were maintained as monolayers in RPMI 1640 medium with L-glutamine (Capricorn Scientific GmbH, Ebsdorfergrund, Germany) supplemented with 10% heat-inactivated fetal bovine serum (Sigma-Aldrich GmbH, Steinheim, Germany) and penicillin/streptomycin (Capricorn Scientific GmbH, Ebsdorfergrund, Germany) at 37 °C in a humidified atmosphere with 5% CO_2.

4.3. Cytotoxicity assay (SRB assay)

For the evaluation of the cytotoxicity of the compounds a sulforhodamine-B (Kiton-Red S, ABCR) micro-culture colorimetric assay was used as previously reported. The EC_{50} values were averaged from three independent experiments performed each in triplicate calculated from semi-logarithmic dose-response curves applying a non-linear 4P Hills-slope equation.

4.4. Microscopic investigation

For the microscopic studies, the cell line A375 was used. On the first day, 10^5 cells were seeded in a Petri dish (3.5 cm diameter, 22 mm cover slip inserted) and incubated under normal conditions for 24 h. The medium was replaced with new medium loaded with **18** (1 μL of an 8 mM solution in 2 mL medium) and incubated for another 24 h. Then the medium was replaced with 1 mL medium loaded with 1 μL Rh123 and 100 μL ER-Tracker ™ red (ER staining Kit - Red Fluorescence, abcam, Milton), respectively, and incubated for 30 min each. The medium was discarded, the cover slip was washed with PBS (with Ca^{2+} and Mg^{2+}) and put on a slide holding 20 μL PBS. The cells were studied using a fluorescence microscope.

4.5. General procedure (GP) for the amidation with acetylated triterpene carboxylic acids chlorides

The acetylated triterpene carboxylic acids **11**–**14** were reacted with oxalyl chloride/DMF as previously reported. They (1 eq.) were dissolved in dry DCM (1 mL), and this solution was added to a solution of **10** (1.2 eq.) and triethylamine (1.2 eq.) under stirring and argon atmosphere. After stirring overnight, the reaction was quenched with MeOH, and the solvents were removed under reduced pressure. The crude product was purified by gradient column chromatography (SiO_2, $CHCl_3$ → $CHCl_3$/MeOH/NH_4OH, 98:1.8:0.2).

*4.6. (E)-1-(4-hydroxyphenyl)-3-phenylprop-2-en-1-one (**2**) [38239-52-0]*

4-Hydroxyacetophenone (**1**, 10.0 g, 73.4 mmol) was dissolved in ethanol (50 mL) and water (150 mL) was added. Under stirring an aqueous solution of sodium hydroxide (50%, 7.4 mL) was added. Stirring was continued for 0.5 h followed by the dropwise addition of benzaldehyde (8.51 mL, 84.2 mmol). After complete consumption of **1** (as checked by TLC), the reaction was acidified with aqueous HCl (10% vol). The precipitate was filtered off, washed with water, recrystallized from ethanol, and dried to obtain **2** (15.3 g, 93%) as an off-white solid; m.p. 177.1 °C (lit.: [33]: 178 °C); R_F = 0.27 (toluene/ethyl acetate/heptane/HCOOH, 80:26:10:5); IR (ATR): $\tilde{\nu}$ = 3125*w*, 1645 *m*, 1602*s*, 1590*s*, 1577 *m*, 1565*s*, 1514 *m*, 1495 *m*, 1441 *m*, 1383*w*, 1339*s*, 1303*w*, 1284*s*, 1219*vs*, 1175*s*. 1165*s*, 1043 *m*, 1028*w*, 999*w*, 980 *m*, 893*w*, 866*w*, 834 m, 823 *m*, 786 *w*, 764*s*, 734 *m*, 691*s*, 674*s*, 638*w*, 620 *m*, 560*s*, 538 *m*, 504 *m*, 482 *m*, 444*w*, 418*w* cm^{-1}; UV/vis ($CHCl_3$): λ_{max} (log ε) = 314 (4.39) nm; ^1H NMR (400 MHz, DMSO-d_6): δ = 10.39 (s, 1H, 1-OH), 8.11–8.03 (m, 2H, 3-H+3′-H), 7.88 (dd, J = 15.5, 2.5 Hz, 1H, 6-H), 7.85–7.81 (m, 2H, 10-H+10′-H), 7.67 (d, J = 15.5 Hz, 1H, 7-H), 7.48–7.37 (m, 3H, 9-H, 9′-H), 6.93–6.86 (m, 2H, 2-H+2′-H) ppm; ^{13}C NMR (101 MHz, DMSO-d_6): δ = 187.6 (C-5), 162.7 (C-1), 143.1 (C-7), 135.3 (C-8), 131.6 (C-3+C-3′), 130.7 (C-11), 129.6 (C-4), 129.3 (C-9+C-9′), 129.1 (C-10+C-10′), 122.6 (C-6), 115.8 (C-2+C-2′) ppm; MS (ESI, MeOH/$CHCl_3$, 4:1): m/z = 223.1 (100%, [M − H]$^-$).

*4.7. 1-(4-Hydroxyphenyl)-4-nitro-3-phenylbutan-1-one (**3**) [1093881-86-7]*

Compound **2** (15.2 g, 67.8 mmol) was dissolved in methanol (500 mL) and nitromethane (72.8 mL, 1.4 mol). Potassium hydroxide (5.0 g, 88.1 mmol) was added in several portions, and the reaction mixture was

heated under reflux for 6 h. The reaction was cooled to room temperature, and the solvent was removed under reduced pressure. The oily residue was acidified with aqueous HCl (1 M, 50 mL) and diluted with water (200 mL). The mixture was extracted with ethyl acetate (200 mL), dried ($MgSO_4$), and the organic solvent was removed under reduced pressure. The residue was purified by column chromatography (SiO_2, hexane/acetone, 4:1) and crystallized from hexanes/acetone (4:1, 200 mL) at 0 °C to obtain **3** (12.4 g, 64%) as a beige solid; m.p. 121.1 °C (lit.: [34]: 112–113 °C); R_F = 0.55 (hexanes/acetone, 2:1); IR (ATR): $\tilde{\nu}$ = 3211*w*, 1646*s*, 1600 *m*, 1585*s*, 1554*vs*, 1515*w*, 1496*w*, 1455 *m*, 1441 *m*, 1430 *m*, 1418 *m*, 1375*s*, 1324*w*, 1288*s*, 1278 *m*, 1230*s*, 1212 *m*, 1169*vs*, 1119*w*, 1078*w*, 1032*w*, 1008 *m*, 1000 *m*, 942*vw*, 921*w*, 891*w*, 838*s*, 819*w*, 798 *m*, 767 *m*, 738 *m*, 720 *m*, 703*s*, 635 *m*, 607*w*, 596 *m*, 543 *m*, 525 *m*, 516 *m*, 492*w*, 446*vw*, 408*w* cm^{-1}; UV/vis ($CHCl_3$): λ_{max} (log ε) = 269 (4.21) nm; ^{1}H NMR (400 MHz, DMSO-d_6): δ = 10.36 (s, 1H, 1-OH), 7.86–7.78 (m, 2H, 3-H+3′-H), 7.40–7.32 (m, 2H, 10-H+10′-H), 7.33–7.25 (m, 2H, 11-H+11′-H), 7.25–7.17 (m, 1H, 12-H), 6.83 (d, J = 8.7 Hz, 2H, 2-H+2′-H), 4.96 (dd, J = 12.9, 5.7 Hz, 8-H_a), 4.85 (dd, J = 12.9, 9.6 Hz, 1H, 8-H_b), 4.02 (ddd, J = 9.6, 6.8 Hz, 1H, 7-H), 3.41 (ddd, J = 17.6, 7.0 Hz, 3H, 6-H_2) ppm; ^{13}C NMR (101 MHz, DMSO-d_6): δ = 195.4 (C-5), 162.2 (C-1), 140.2 (C-9), 130.5 (C-3+C-3′), 128.4 (C-11+C-11′), 128.1 (C-4), 127.8 (C-10+C-10′), 127.1 (C-12), 115.2 (C-2+C-2′), 79.7 (C-8), 40.6 (C-6), 39.4 (C-7) ppm; MS (ESI, $CHCl_3$/MeOH, 4:1): m/z = 284.0 (30%, $[M - H]^-$).

4.8. 4-Cinnamoylbenzoic acid (5) [20118-35-8]

To a suspension of 4-acetylbenzoic acid (**4**, 10.0 g, 61 mmol) in ethanol (200 mL) and water (50 mL) was added dropwise aqueous potassium solution (6 M, 32 mL) under stirring at room temperature. Benzaldehyde (6.5 g, 61 mmol) was added dropwise, and the reaction mixture was allowed to stir overnight [35]. The white suspension was acidified with aqueous HCl (1 M), the solid filtered off, washed with water (3 × 100 mL), air-dried, and recrystallized from ethanol to yield **5** (13.8 g, 90%) as a white solid; m.p. 237.1 °C (lit.: [36]: 234 °C); R_F = 0.37 (toluene/ethyl acetate/heptane/HCOOH, 80:26:10:5); IR (ATR): $\tilde{\nu}$ = 2663*w*, 2546*w*, 1685 *m*, 1655 *m*, 1595 *m*, 1574 *m*, 1506*w*, 1497*w*, 1448*w*, 1426 *m*, 1406*w*, 1336 *m*, 1322 *m*, 1283*s*, 1216 *m*, 1206 *m*, 1183*w*, 1128 *m*, 1033 *m*, 1014 *m*, 996 *m*, 978 *m*, 969 *m*, 944 *m*, 854 *m*, 849 *m*, 778 *m*, 749*vs*, 709*w*, 686*s*, 662 *m*, 572 *m*, 558 *m*, 519 *m*, 488 *m*, 482 *m*, 447*w* cm^{-1}; UV/vis (MeOH): λ_{max} (log ε) = 313 (4.05), 265 (3.88) nm; ^{1}H NMR (400 MHz, DMSO-d_6): δ = 13.31 (s, 1H, 1-OH), 8.23 (dd, J = 8.3, 1.6 Hz, 2H, 3-H+3′H), 8.11–8.06 (m, 5H, 4-H+4′-H), 7.91 (d, J = 1.3 Hz, 1H, 7-H), 7.89 (ddd, J = 5.7, 2.8, 1.5 Hz, 2H, 10-H+10′-H), 7.77 (d, J = 15.7 Hz, 1H, 8-H), 7.49–7.44 (m, 3H, 11-H+11′-H+12-H) ppm; ^{13}C NMR (126 MHz, DMSO-d_6): δ = 189.0 (C-6), 166.6 (C-1), 144.8 (C-8), 140.7 (C-5), 134.5 (C-9), 134.4 (C-2), 130.8 (C-12), 129.6 (C-4+C-4′), 129.0 (C-10+C-10′), 128.9 (C-11+C-11′), 128.6 (C-3+C-3′), 122.0 (C-7) ppm; MS (ESI, $CHCl_3$/MeOH, 4:1): m/z = 250.9 (100%, $[M - H]^-$), 386.8 (40%, $[M+Cl]^-$).

4.9. 4-(4-Nitro-3-phenylbutanoyl)benzoic acid (6) [1815579-07-7]

To a suspension of **5** (7.1 g, 28.1 mmol) in methanol (500 mL) and nitromethane (30.2 mL, 0.3 mol), potassium hydroxide (2.07 g, 36.9 mmol) was added in several portions. The reaction was stirred and heated under reflux for 6 h, and the solvent was removed under reduced pressure. The residue was treated with aqueous HCl solutions (0.1 M, 200 mL; 1 M, 10 mL) and ethyl acetate (200 mL). The organic phase was separated, dried ($MgSO_4$), and the solvent was removed under reduced pressure to yield **6** (8.65 g, 98%) as a beige solid; m.p. 175.1 °C; R_F = 0.31 (toluene/ethyl acetate/heptane/HCOOH, 80:26:10:5); IR (ATR): $\tilde{\nu}$ = 3101*w*, 3062*w*, 3032*w*, 2897*w*, 2666*w*, 2550*w*, 1696*s*, 1682*vs*, 1571*w*, 1549*vs*, 1506*w*, 1454*w*, 1424 *m*, 1406 *m*, 1378 *m*, 1367*w*, 1322 *m*, 1291*s*, 1220 *m*, 1202 *m*, 1128*w*, 1119*w*, 992*w*, 976*w*, 971*w*, 930*w*, 853 *m*, 806*w*, 769 *m*, 757 *m*, 700*s*, 683*w*, 643*w*, 557 *m*, 509*w* cm^{-1}; UV/vis (MeOH): λ_{max} (log ε) = 294 (3.22), 253 (4.22) nm; ^{1}H NMR (400 MHz, DMSO-d_6): δ = 13.29 (s, 1H, 1-OH), 8.06–7.96 (m, 4H, 3-H+3′-H+4-H+4′-H), 7.38–7.33 (m, 2H, 11-H+11′-H), 7.32–7.25 (m, 2H, 12-H+12′-H), 7.24–7.18 (m, 1H, 13-H), 4.97 (dd, J = 13.0, 5.7 Hz, 1H, 9-H_a), 4.84 (dd, J = 12.9, 9.6 Hz, 1H, 9-H_b), 4.03 (dq, J = 9.6, 6.9 Hz, 1H, 8-H), 3.67–3.50 (m, 2H, 7-H_2) ppm; ^{13}C NMR (126 MHz, DMSO-d_6): δ = 197.7 (C-6), 167.0 (C-1), 140.4 (C-10), 139.9 (C-5), 135.1 (C-2), 130.0 (C-4+C-4′), 128.9 (C-12+C-12′), 128.6 (C-3+C-3), 128.2 (C-11+C-11′), 127.7 (C-13), 80.1 (C-9), 42.0 (C-7), 39.6 (C-8) ppm; MS (ESI, $CHCl_3$/MeOH, 4:1): m/z = 312.0 (100%, $[M - H]^-$; analysis calcd for $C_{17}H_{15}NO_5$ (313.31): C 65.17, H 4.83, N 4.47; found: C 64.79, H 5.03, N 4.20.

4.10. tert-Butyl 4-[4-(4-nitro-3-phenylbutanoyl)benzoyl]piperazine carboxylate (7)

Compound **6** (6.0 g, 19.2 mmol) was suspended in dry DCM (50 mL) under argon atmosphere. The suspension was cooled to 0 °C, and under stirring cat. amounts of dry DMF and oxalyl chloride (3.2 mL, 38.3 mmol) were added. The solution was stirred for 1.5 h at 21 °C; the solvent was removed under reduced pressure. The obtained acid chloride was redissolved in dry THF (2 × 100 mL), and the solvent was removed multiple times to remove excessive oxalyl chloride. The acid chloride was taken up in dry DCM (5 mL) and transferred dropwise to a solution of N-Boc-piperazine (3.9 g, 21.1 mmol), and triethylamine (0.9 mL, 21.1 mmol) in dry DCM (10 mL). After stirring for 2 h, the solvent was removed under reduced pressure, and the beige solid was purified by column chromatography (SiO_2, hexanes/ethyl acetate, 2:1) to yield **7** (6.64 g, 72%) as a white solid; m.p. 63.2 °C; R_F = 0.36 (hexanes/ethyl acetate, 2:1); IR (ATR): $\tilde{\nu}$ = 2976*w*, 2864*w*, 1685*s*, 1631*s*, 1549*s*, 1505*w*, 1456 *m*, 1416*s*, 1378 *m*, 1365*s*, 1286 *m*, 1262*s*, 1247*vs*, 1231*s*, 1207 *m*, 1155*vs*, 1119*s*, 1075*w*, 1006*s*, 997*s*, 893*w*, 842 *m*, 759*s*, 700*s*, 551 m cm^{-1}; UV/vis ($CHCl_3$): λ_{max} (log ε) = 255 (4.12) nm; ^{1}H NMR (500 MHz, $CDCl_3$): δ = 7.98–7.93 (m, 2H, 4-H+4′-H), 7.50–7.43 (m, 2H, 3-H+3′-H), 7.35–7.30 (m, 2H, 12-H+12′-H), 7.29–7.24 (m, 3H, 11-H+11′-H+13-H), 4.85–4.78 (m, 1H, 7-H_a), 4.73–4.66 (m, 1H, 7-H_b), 4.21 (p, J = 7.1 Hz, 1H, 8-H), 3.74 (s, 2H, 14-H_a+15-H_a), 3.61–3.25 (m, 8H, 9-H_2+14-H_b+14′-H_2+15-H_2+15′-H_2), 1.46 (s, 9H, 18-H_3+18′-H_3+18″-H_3) ppm; ^{13}C NMR (126 MHz, $CDCl_3$): δ = 196.3 (C-6), 169.3 (C-1), 154.6 (C-16), 140.4 (C-2), 139.0 (C-10), 137.4 (C-5), 129.2 (C-12+C-12′), 128.5 (C-4+C-4′), 128.1(C-13), 127.6 (C-11+C-11′), 127.5(C-3+C-3′), 80.6 (C-17), 79.6 (C-7), 47.1 (C-14+C-14′), 42.0 (C-15+C-15′), 41.8 (C-9), 39.4 (C-8), 28.5 (C-18+C-18'+C-18″) ppm; MS (ESI, $CHCl_3$/MeOH, 4:1): m/z = 504.2 (100%, $[M+Na]^+$); analysis calcd for $C_{26}H_{31}N_3O_6$ (481.55): C 64.85, H 6.49, N 8.73; found: C 64.69, H 6.71, N 8.55.

4.11. tert-butyl (Z)-4-(4-{2-([5-(4-hydroxyphenyl)-3-phenyl-1H-pyrrol-2-yl]imino}-3-phenyl-2H-pyrrol-5-yl)benzoyl)piperazine-1-carboxylate (8)

Compounds **3** (1.86 g, 6.5 mmol), **7** (3.14 g, 6.5 mmol), and ammonium acetate (17.6 g, 228 mmol) were dissolved in *n*-butanol (50 mL), and the mixture was stirred under reflux for 8 h. The solvent was removed under reduced pressure, and the blue solid was washed with water, filtered off and dissolved in DCM (100 mL). The organic phase was washed with small amounts of water until pH neutral. After drying ($MgSO_4$), the compound was purified by column chromatography (SiO_2, $CHCl_3$/ethyl acetate, 9:2) to afford **8** (3.68 g, 54%) as a blue solid; m.p. 223.6 °C; R_F = 0.41 ($CHCl_3$/MeOH/NH_4OH, 98:1.8:0.2); IR (ATR): $\tilde{\nu}$ = 1690*s*, 1600*s*, 1587 *m*, 1562 *m*, 1465*s*, 1419*s*, 1291 *m*, 1277 *m*, 1263*s*, 1235*vs*, 1219 *m*, 1163*vs*, 1122*s*, 1005*vs*, 848*s*, 824*s*, 768*s*, 758*vs*, 694*s*, 550 m cm^{-1}; UV/vis ($CHCl_3$): λ_{max} (log ε) = 602 (4.31), 317 (4.53) nm; ^{1}H NMR (500 MHz, DMSO-d_6): δ = 12.70 (s, 1H, 5-NH), 11.54 (t, J = 2.8 Hz, 1H, 1-OH), 8.13–8.10 (m, 2H, 22-H+22′-H), 8.10–8.04 (m, 2H, 15-H+15′-H), 7.80 (s, 1H, 19-H), 7.75–7.70 (m, 2H, 2-H+2′-H), 7.63–7.58 (m, 3H, 10-H+10′-H+13-H), 7.48–7.43 (m, 2H, 14-H+14′-H), 7.43–7.40 (m, 2H, 23-H+23′-H), 7.40–7.37 (m, 2H, 3-H+3′-H), 7.35–7.28 (m, 2H, 11-H+11′-H), 7.15–7.09 (m, 1H, 12-H), 7.05–7.03 (m, 1H, 6-H),

3.64–3.30 (m, 8H, 26-H_2+26′-H_2+27-H_2+27′-H_2), 1.40 (s, 9H, 30 + 30′-H_3+30″-H_3) ppm; ^{13}C NMR (126 MHz, DMSO-d_6): δ = 169.6 (C-25), 169.2 (C-1), 167.0 (C-20), 158.0 (C-17), 154.3 (C-28), 146.7 (C-21), 142.0 (C-18), 136.0 (C-9), 134.4 (C-24), 133.3 (C-16), 132.3 (C-7), 131.9 (C-4), 131.1 (C-22+C-22′), 129.3 (C-15+C-15′), 129.0 (C-11+C-11′), 128.7 (C-13+C-14+C-14′), 128.3 (C-23+C-23′), 125.6 (C-5), 125.5 (C-8), 125.4 (C-12), 124.9 (C-10+C-10′), 123.5 (C-2+C-2′), 122.1 (C-19), 117.9 (C-3+C-3′), 104.7 (C-6), 79.6 (C-29), 47.4 (C-26+C-26′), 44.1 (C-27+C-27′), 28.5 (C-30+C-30'+C-30″) ppm; MS (ESI, $CHCl_3$/MeOH, 4:1): m/z = 676.3 (70%, [M − H]$^-$); analysis calcd for $C_{42}H_{39}N_5O_4$ (677.81): C 74.43, H 5.80, N 10.33; found: C 74.17, H 6.03, N 10.03.

4.12. 3-(4-Hydroxyphenyl)-1,7-diphenyl-5-{4-[4-(tert-butoxycarbonyl) piperazine-1-carbonyl] phenyl}-4,4-difluoro-4-bora-3a,4a,8-triaza-s-indacene (9)

To an ice-cold solution of **8** (2.45 g, 3.6 mmol) in dry DCM (200 mL), boron trifluoride diethyl etherate (4.58 mL, 36 mmol) and DIPEA (6.15 mL, 36 mmol) were added dropwise under stirring. The green solution was stirred overnight and quenched with an aqueous solution of $NaHCO_3$ (20 mL, satd.). The mixture was filtered through a pad of Celite, which was rinsed with ethyl acetate until no green color was observed. The organic phase was separated, washed with water (20 mL), brine (20 mL), and dried over $MgSO_4$. Once the solvent was removed under reduced pressure, the green solid was purified by column chromatography (SiO_2, $CHCl_3$ → $CHCl_3$:MeOH:NH_4OH, 9:1.8:0.2) to obtain unchanged starting material **8** (490 mg, 20%), product **9** (1144 mg, 44%) and deprotected **10** (522 mg, 23%); m.p. 256 °C; R_F = 0.28 ($CHCl_3$/ethyl acetate, 4:1); IR (ATR): $\tilde{\nu}$ = 3397*w*, 3007*w*, 2977*w*, 2927*w*, 2868*w*, 2257*vw*, 1686 *m*, 1616 *m*, 1604 *m*, 1538 *m*, 1506*s*, 1475*s*, 1461*s*, 1444*s*, 1421*s*, 1389 *m*, 1365 *m*, 1323 *m*, 1285*s*, 1247*s*, 1233*s*, 1177*s*, 1121*s*, 1100*s*, 1071*s*, 1051 *m*, 1033*s*, 1021*vs*, 1006*vs*, 863 *m*, 820*s*, 761*s*, 744 *m*, 689*s*, 619*s*, 540 m cm^{-1}; UV/vis ($CHCl_3$): λ_{max} (log ε) = 669 (4.04), 467 (3.20), 320 (3.63) nm; ^{1}H NMR (500 MHz, DMSO-d_6): δ = 8.29 (s, 1H, 1-OH), 8.24–8.16 (m, 4H, 3-H+3′-H+11-H+11′-H), 8.14–8.08 (m, 4H, 14-H+14′-H+22-H+22′-H), 7.80 (s, 1H, 6-H), 7.58–7.47 (m, 7H, 10-H+10′-H+12-H+15-H+15′-H+23-H+23′-H), 7.46–7.40 (m, 2H, 13-H+19-H), 6.99–6.96 (m, 2H, 2-H+2′-H), 3.48–3.23 (m, 8H, 26-H_2+26′-H_2+27-H_2+27′-H_2), 1.40 (s, 9H, 30-H_3+30′-H_3+30-H″-H_3) ppm; ^{13}C NMR (126 MHz, DMSO-d_6): δ = 169.0 (C-25), 163.0 (C-1), 162.4 (C-5), 154.3 (C-28), 153.2 (C-16), 146.9 (C-8), 144.8 (C-9), 143.5 (C-17), 140.3 (C-20), 137.3 (C-24), 133.8 (C-3+C-3′), 133.2 (C-21), 132.7 (C-18), 131.7 (C-7), 130.6 (C-12), 129.8 (C-11+C-11′), 129.6 (C-22+C-22′), 129.5 (C-13), 129.4 (C-14+C-14′), 129.2 (C-15+C-15′), 129.1 (C-10+C-10′), 127.7 (C-23+C-23′), 122.3 (C-6), 121.2 (C-4), 118.9 (C-19), 116.7 (C-2+C-2′), 79.7 (C-29), 45.8 (C-26+C-26′), 41.0 (C-27+C-27′), 28.5 (C-30+C-30'+C-30″) ppm; MS (ESI, MeOH): m/z = 724.3 (100%, [M − H]$^-$); analysis calcd for $C_{42}H_{38}BF_2N_5O_4$ (725.59): C 69.52, H 5.28, N 9.65; found: C 69.36, H 5.47, N 9.38.

4.13. 3-(4-Hydroxyphenyl)-1,7-diphenyl-5-(4-(piperazine-1-carbonyl) phenyl)-4,4-difluoro-4-bora-3a,4a,8-triaza-s-indacene (10)

Compound **9** (720 mg, 1 mmol) was dissolved in methanol (15 mL) and HCl solution in dioxane (4 M, 10 mL, 1.1 mmol) was added under stirring. After consumption of the starting material (as checked by TLC), the solvent was removed under reduced pressure, and the solid residue was purified by column chromatograhpy (SiO_2, $CHCl_3$/MeOH/NH_4OH, 90:9:1) to afford **10** (570 mg, 91%) as a green solid; m.p. 200 °C; R_F = 0.17 ($CHCl_3$/MeOH/NH_4OH, 90:9:1); IR (ATR): $\tilde{\nu}$ = 1633*w*, 1596 *m*, 1539 *m*, 1512 *m*, 1504 *m*, 1415*s*, 1364 *m*, 1319 *m*, 1280*s*, 1232*s*, 1178 *m*, 1126*s*, 1094*s*, 1068*s*, 1035*s*, 1021*vs*, 983*s*, 962*s*, 939*s*, 865 *m*, 822*s*, 760*vs*, 744*s*, 714 *m*, 686*vs*, 617*s*, 566*s*, 552*s*, 530*s*, 462*s*, 403 s cm^{-1}; UV/vis ($CHCl_3$): λ_{max} (log ε) = 669 (4.91), 467 (4.07), 319 (4.50) nm; ^{1}H NMR (500 MHz, $CDCl_3$): δ = 8.17–7.95 (m, 7H, 3-H+3′-H+11-H+11′-H+12-H+14-H-14′-H), 7.56–7.32 (m, 9H, 10-H+10′-H+13-H+15-H+15′-H+22-H+22′-H+23-H+23′-H), 7.16 (s, 1H, 19-H), 6.94–6.79 (m, 3H, 2-H+2′-H+6-H), 3.94–3.08 (m, 8H, 26-H_2+26′-H_2+27-H_2+27′-H_2) ppm; ^{11}B NMR (160 MHz, $CDCl_3$): δ = 1.01 (t, J = 31.6 Hz) ppm; ^{19}F NMR (470 MHz, $CDCl_3$): δ = −130.85–132.06 (m) ppm; MS (ESI, MeOH): m/z = 624.3 (100%, [M − H]$^-$); analysis calcd for $C_{37}H_{30}BF_2N_5O_2$ (625.49): C 71.05, H 4.83, N 11.20; found: C 70.81, H 5.06, N 10.97.

4.14. 3-O-acetyl-glcycyrrhetinic acid (11), 3-O-acetyl-ursolic acid (12), 3-O-acetyl-oleanolic acid (13), 3-O-acetyl-betulinic acid (14)

These compounds were prepared from the parent triterpenoic acids by acetylation as previously described [30].

4.15. 3-(4-Hydroxyphenyl)-1,7-diphenyl-5-{4-[N-(3β-acetyloxy-11-oxo-olean-12-en-28-oyl] piperazine-1-carbonyl)phenyl}-4,4-difluoro-4-bora-3a,4a,8-triaza-s-indacene (15)

Following the GP from **11** (38 mg, 74 μm mol), **15** (58 mg, 70%) was obtained as a green solid; m.p. 287 °C; R_F = 0.15 ($CHCl_3$/MeOH/NH_4OH, 98:1.8:0.2); IR (ATR): $\tilde{\nu}$ = 2947*w*, 2928*w*, 2865*w*, 1728*w*, 1634 *m*, 1603 *m*, 1538 *m*, 1509 *m*, 1483 *m*, 1473 *m*, 1445 *m*, 1417 *m*. 1387 *m*, 1365 *m*, 1320 *m*, 1280 *m*, 1241*s*, 1178*s*, 1126*s*, 1095*s*, 1070*s*, 1036*vs*, 1022*vs*, 1002*vs*, 985*s*, 827 *m*, 761*s*, 746*s*, 688*s*, 673 *m*, 617 *m*, 407 m cm^{-1}; UV/vis ($CHCl_3$): λ_{max} (log ε) = 669 (4.88), 469 (4.05), 320 (4.43) nm; ^{1}H NMR (500 MHz, $CDCl_3$): δ = 8.08–7.98 (m, 7H, 46-H+46′-H+47-H+53-H+53′-H+58-H+58′-H), 7.57–7.33 (m, 9H, 37-H+37′-H+38-H+38′-H+45-H+45′-H+57-H+57′-H+59-H), 7.12 (s, 1H, 50-H), 6.97–6.88 (m, 3H, 41-H+54-H+54′-H), 5.68 (s, 1H, 12-H), 4.49 (dd, J = 11.7, 4.7 Hz, 1H, 3-H), 3.93–3.41 (m, 8H, 33-H_2+33′-H_2+34-H_2+34′-H_2), 2.79 (d, J = 13.4 Hz, 1H, 1-H_a), 2.37 (s, 1H, 9-H), 2.23 (d, J = 13.1 Hz, 1H, 18-H), 2.07 (s, 3H, 32-H_3), 2.13–2.01 (m, 2H, 16-H_a+19-H_a), 2.01–1.94 (m, 1H, 21-H_a), 1.88–1.78 (m, 1H, 15-H_a), 1.78–1.38 (m, 10H, 2-H_2+6-H_2+7-H_2+19-H_b+21-H_a+22-H_2), 1.36 (s, 3H, 27-H_3), 1.23 (s, 3H, 29-H_3), 1.22–1.15 (m, 1H, 15-H_b), 1.17 (s, 3H, 25-H_3), 1.12 (s, 3H, 26-H_3), 1.10–0.99 (m, 2H, 1-H_b+16-H_b), 0.91–0.87 (m, 6H, 23-H_3+24-H_3), 0.82 (s, 3H, 28-H_3), 0.85–0.74 (m, 1H, 5-H) ppm; ^{11}B NMR (160 MHz, $CDCl_3$): δ = 0.99 (t, J = 31.0 Hz) ppm; ^{19}F NMR (376 MHz, $CDCl_3$): δ = −130.15–132.95 (m) ppm; ^{13}C NMR (126 MHz, $CDCl_3$): δ = 200.2 (C-11), 174.5 (C-30), 171.6 (C-31), 170.3 (C-35), 169.8 (C-13), 161.9 (C-51), 160.7 (C-55), 154.1 (40), 146.9 (C-49), 145.2 (C-56), 141.5 (C-42), 135.8 (C-36), 134.1 (C-39), 132.7 (C-47), 132.6 (C-43), 131.8 (C-44), 129.8 (C-59), 129.7 (C-48), 129.4 (C-58+C-58'+C-53+C-53′), 129.2 (C-46+C-46′), 129.0 (C-37+C-37′), 128.6 (C-57+C-57′), 128.5 (C-45+C-45′), 128.3 (C-12), 127.3 (C-38+C-38′), 122.6 (C-52), 120.2 (C-50), 117.9 (C-41), 116.3 (C-51+C-51′), 81.2 (C-3), 61.8 (C-9), 55.0 (C-5), 48.5 (C-18), 47.7 (C-34+C-34′), 45.4 (C-8), 43.9 (C-20), 43.5 (C-21), 43.4 (C-14), 42.5 (C-33+C-33′), 38.8 (C-1), 38.0 (C-4), 37.6 (C-22), 36.9 (C-10), 33.5 (C-19), 32.8 (C-7), 31.9 (C-17), 28.4 (C-28), 28.0 (C-24), 27.1 (C-29), 26.7 (C-16), 26.4 (C-15), 23.5 (C-2), 23.1 (C-27), 21.4 (C-32), 18.7 (C-26), 17.4 (C-6), 16.7 (C-23), 16.4 (C-25) ppm; MS (ESI, $CHCl_3$/MeOH, 4:1): m/z = 1119.3 (100%, [M]$^-$); analysis calcd for $C_{69}H_{76}BF_2N_5O_6$ (1120.20): C 73.98, H 6.84, N 6.25; found: C 73.60, H 7.02, N 6.02.

4.16. 3-(4-Hydroxyphenyl)-1,7-diphenyl-5-{4-[N-(3β-acetyloxy-ursan-12-en-28-oyl] piperazine-1-carbonyl)phenyl)}-4,4-difluoro-4-bora-3a,4a,8-triaza-s-indacene (16)

Following the GP from **12** (30 mg, 58 μm mol), **13** (41 mg, 63%) was obtained as a green solid; m.p. 234 °C; R_F = 0.27 ($CHCl_3$/MeOH/NH_4OH, 98:1.8:0.2); IR (ATR): $\tilde{\nu}$ = 2923*w*, 2870*w*, 1730*w*, 1634 *m*, 1602 *m*, 1540 *m*, 1511 *m*, 1501 *m*, 1483 *m*, 1475*s*, 1444*s*, 1419 *m*, 1388*s*, 1369 *m*, 1320 *m*, 1281 m, 1237*s*, 1178*s*, 1126*s*, 1095*s*, 1071*s*, 1036*vs*, 1022*vs*, 1003*s*, 985*s*, 968 *m*, 944 *m*, 826 *m*, 771*s*, 746 *m*, 688*s*, 663 *m*, 618 *m*, 579 *m*, 411 m cm^{-1}; UV/vis ($CHCl_3$): λ_{max} (log ε) = 666 (4.89), 471 (4.05), 318 (4.43) nm; ^{1}H NMR (400 MHz, $CDCl_3$): δ = 8.12–7.96 (m, 7H, 46-H+46′-

H+47-H+53-H+53′-H+58-H+58′-H), 7.58–7.31 (m, 9H, 37-H+37′-H+38-H+38′H+45-H+45′-H+57-H+57′-H+59-H), 7.12 (s, 1H, 50-H), 6.98–6.86 (m, 3H, 41-H+54-H+54′-H), 5.20 (s, 1H, 12-H), 4.48 (q, J = 7.8, 6.3 Hz, 1H, 3-H), 3.97–3.18 (m, 8H, 33-H_2+33′-H_2+34-H_2+34′-H_2), 2.46–2.09 (m, 1H, 18-H), 2.03 (s, 3H, 32-H_3), 1.95–1.84 (m, 2H, 11-H_2), 1.83–1.17 (m, 15H, 1-H_a+2-H_2+6-H_2+7-H_2+9-H+16-H_2+19-H+21-H_2+22-H_2), 1.07–0.97 (m, 7H, 1-H_b+15-H_2+20-H+27-H_3), 0.96–0.89 (m, 6H, 25-H_3+30-H_3), 0.89–0.84 (m, 3H, 29-H_3), 0.84–0.75 (m, 7H, 5-H+23-H_3+24-H_3), 0.71 (d, J = 3.9 Hz, 3H, 26-H_3) ppm; ^{11}B NMR (128 MHz, $CDCl_3$): δ = 0.99 (t, J = 31.5 Hz) ppm; ^{19}F NMR (376 MHz, $CDCl_3$): δ = −129.13–134.44 (m) ppm; ^{13}C NMR (101 MHz, $CDCl_3$): δ = 175.9 (C-28), 171.1 (C-31), 170.3 (C-35), 162.1 (C-51), 161.0 (C-55), 153.6 (C-40), 146.9 (C-49), 145.3 (C-56), 141.4 (C-42), 138.5 (C-13), 135.7 (C-36), 134.3 (C-39), 132.7 (C-47), 132.6 (C-43), 131.7 (C-44), 129.8 (C-59), 129.6 (C-48), 129.4 (C-53+C-53′), 129.4 (C-58+C-58′), 129.1 (C-46+C-46′), 129.0 (C-37+C-37′), 128.6 (C-45+C-45′), 128.6 (C-57+C-57′), 127.4 (C-38+C-38′), 125.4 (C-12), 122.3 (C-52), 120.3 (C-50), 117.6 (C-41), 116.4 (C-54+C-54′), 81.0 (C-3), 55.3 (C-5+C-18), 48.7 (C-17), 47.5 (C-9), 45.3 (C-33+C-33'+C-34+C-34′), 42.1 (C-14), 39.4 (C-8+C-19), 38.7 (C-20), 38.2 (C-1), 37.6 (C-4), 36.9 (C-10), 34.4 (C-22), 33.0 (C-7), 30.4 (C-21), 28.1 (C-15), 28.0 (C-24), 23.5 (C-16+C-27), 23.3 (C-11), 21.3 (C-32), 21.2 (C-30), 18.2 (C-2+C-6), 17.4 (C-29), 16.9 (C-26), 16.7 (C-23), 15.5 (C-25) ppm; MS (ESI, $CHCl_3$/MeOH, 4:1): m/z = 1106.3 (40%, $[M]^-$); analysis calcd for $C_{69}H_{78}BF_2N_5O_5$ (1106.22): C 74.92, H 7.11, N 6.33; found: C 74.68, H 7.40, N 6.01.

*4.17. 3-(4-Hydroxyphenyl)-1,7-diphenyl-5-{4-[N-(3β-acetyloxy-olean-12-en-28-oyl] piperazine-1-carbonyl)phenyl}-4,4-difluoro-4-bora-3a,4a,8-triaza-s-indacene (**17**)*

Following the GP from **13** (30 mg, 58 μm mol), **15** (30 mg, 47%) was obtained as a green solid; m.p. 283 °C; R_F = 0.23 ($CHCl_3$/MeOH/NH_4OH, 98:1.8:0.2); IR (ATR): $\tilde{\nu}$ = 2942*w.* 2927*w,* 2866*w,* 1729*w,* 1629 *m,* 1602 *m,* 1539 *m,* 1510 *m,* 1501 *m,* 1483 *m,* 1473*s,* 1444*s,* 1418 *m,* 1387*s,* 1366 *m,* 1320 *m,* 1279*s,* 1237*s,* 1178*s,* 1124*s,* 1094*vs,* 1070*s,* 1036*s,* 1021*vs,* 1001*vs,* 985*s,* 968*s,* 943 *m,* 916 *m,* 826 *m,* 760*s,* 746*s,* 714 *m,* 687*s,* 665 *m,* 617 *m,* 586 *m,* 574 *m,* 531 *m,* 408 m cm^{-1}; UV/vis ($CHCl_3$): λ_{max} (log ε) = 667 (4.93), 471 (4.09), 319 (4.49) nm; ^{1}H NMR (500 MHz, $CDCl_3$): δ = 8.13–7.94 (m, 7H, 46-H+46′-H+47-H+53-H+53′-H+58-H+58′-H), 7.51–7.30 (m, 9H, 37-H+37′-H+38-H+38′-H+45-H+45′-H+57-H+57′-H+59-H), 7.09 (s, 1H, 50-H), 6.96 (d, J = 8.2 Hz, 2H, 54-H+54′-H), 6.93 (s, 1H, 41-H), 5.24 (t, J = 3.7 Hz, 1H, 12-H), 4.46 (t, J = 7.9 Hz, 1H, 3-H), 3.87–3.27 (m, 8H, 33-H_2+33′-H_2+34-H_2+34′-H_2), 3.10–2.99 (m, 1H, 18-H), 2.16–1.98 (m, 1H, 16-H_a), 2.03 (s, 3H, 32-H_3), 1.96–1.77 (m, 2H, 11-H_2), 1.74–1.42 (m, 10H, 1-H_a+2-H_2+6-H_a+9-H+15-H_a+16-H_b+19-H_a+22-H_2), 1.42–1.12 (m, 6H, 6-H_b+7-H_2+19-H_b+21-H_2), 1.09 (s, 3H, 27-H_3), 1.07–0.96 (m, 2H, 1-H_b+15-H_b), 0.90 (s, 3H, 29-H_3), 0.89 (s, 3H, 25-H_3), 0.87 (s, 3H, 30-H_3), 0.82 (s, 3H, 24-H_3), 0.80 (s, 3H, 23-H_3), 0.80–0.76 (m, 1H, 5-H), 0.70 (s, 3H, 26-H_3) ppm; ^{11}B NMR (128 MHz, $CDCl_3$): δ = 0.97 (t, J = 31.4 Hz) ppm; ^{19}F NMR (470 MHz, $CDCl_3$): δ = −129.19–-133.50 (m) ppm; ^{13}C NMR (126 MHz, $CDCl_3$): δ = 175.6 (C-28), 171.1 (C-31), 170.2 (C-35), 162.2 (C-55), 161.4 (C-51), 153.3 (C-40), 146.9 (C-49), 145.3 (C-56), 144.4 (C-13), 143.9 (C-42), 135.8 (C-36), 134.2 (C-39), 132.7 (C-47), 132.6 (C-43), 131.6 (C-44), 129.8 (C-59), 129.6 (C-48), 129.4 (C-53+C-53′), 129.4 (C-58+C-58′), 129.1 (C-46+C-46′), 129.0 (C-37+C-37′), 128.6 (C-45+C-45′), 128.6 (C-57+C-57′), 127.3 (C-38+C-38′), 122.1 (C-12), 121.7 (C-52), 120.3 (C-50), 117.5 (C-41), 116.5 (C-54+C-54′), 81.0 (C-3), 55.4 (C-5), 47.6 (C-9), 47.6 (C-17), 46.3 (C-19), 45.3 (C-34+C-34′), 43.6 (C-18), 42.4 (C-33+C-33′), 41.8 (C-8), 39.1 (C-14), 38.1 (C-1), 37.7 (C-4), 36.9 (C-10), 33.9 (C-21), 33.0 (C-30), 32.8 (C-7), 30.3 (C-20), 30.0 (C-22), 28.0 (C-24), 27.8 (C-15), 25.9 (C-27), 24.0 (C-29), 23.5 (C-2), 23.4 (C-11), 22.8 (C-16), 21.3 (C-32), 18.2 (C-6), 16.9 (C-26), 16.6 (C-23), 15.4 (C-25) ppm; MS (ESI, $CHCl_3$/MeOH, 4:1): m/z = 1105.4 (100%, $[M]^-$); analysis calcd for $C_{69}H_{78}BF_2N_5O_5$ (1106.22): C 74.92, H 7.11, N 6.33; found: C 74.77, H 7.34, N 6.02.

*4.18. 3-(4-Hydroxyphenyl)-1,7-diphenyl-5-{4-[N-(3β-acetyloxy-lup-20(29)en-28-oyl] piperazine-1-carbonyl)phenyl}-4,4-difluoro-4-bora-3a,4a,8-triaza-s-indacene (**18**)*

Following the GP from **14** (50 mg, 58 μm mol), **17** (55 mg, 50%) was obtained as a green solid; m.p. 274 °C; R_F = 0.25 ($CHCl_3$/MeOH/NH_4OH, 98:1.8:0.2); IR (ATR): $\tilde{\nu}$ = 2941 *m,* 2867*w,* 1729*w,* 1635 *m,* 1602 *m,* 1537 *m,* 1511 *m,* 1505 *m,* 1502 *m,* 1483 *m,* 1474*s,* 1445*s,* 1418 *m,* 1388*s,* 1372 *m,* 1320 *m,* 1281*s,* 1262 *m,* 1238*s,* 1179*s,* 1125*s,* 1095*s,* 1070*s,* 1036*vs,* 1022*vs,* 1002*vs,* 979*s,* 944 *m,* 916 *m,* 899 *m,* 865 *m,* 841 *m,* 826 *m,* 771*s,* 763*s,* 746*s,* 713 *m,* 688*s,* 617 *m,* 587 *m,* 577 *m,* 530 *m,* 409 m cm^{-1}; UV/vis ($CHCl_3$): λ_{max} (log ε) = 667 (4.89), 472 (4.05), 318 (4.47) nm; ^{1}H NMR (500 MHz, $CDCl_3$): δ = 8.08–8.01 (m, 7H, 46-H+46′-H+47-H+53-H+53-H+58-H+58′-H), 7.55–7.36 (m, 9H, 37-H+37′-H+38-H+38′-H+45-H+45′-H+57-H+57′-H+59-H), 7.10 (s, 1H, 50-H), 6.95 (s, 1H, 41-H), 6.89 (d, J = 8.3 Hz, 2H, 54-H+54′-H), 4.74–4.67 (m, 1H, 29-H_a), 4.58 (d, J = 2.0 Hz, 1H, 29-H_b), 4.49–4.40 (m, 1H, 3-H), 3.86–3.32 (m, 8H, 33-H_2+33′-H_2+34-H_2+34′-H_2), 3.01–2.90 (m, 1H, 19-H), 2.86–2.75 (m, 1H, 13-H), 2.03 (s, 3H, 32-H_3), 2.06–1.96 (m, 1H, 16-H_a), 1.96–1.77 (m, 2H, 21-H_a+22-H_a), 1.66 (s, 3H, 30-H_3), 1.72–1.49 (m, 6H, 1-H_a+2-H_2+9-H+12-H_a+16-H_b), 1.48–1.19 (m, 10H, 6-H_2+7-H_2+11-H_2+15-H_a+21-H_b+22-H_b+18), 1.12 (d, J = 13.2 Hz, 1H, 15-H_b), 0.99–0.83 (m, 2H, 1-H_b+12-H_b), 0.92 (s, 3H, 27-H_3), 0.89 (s, 3H, 26-H_3), 0.81 (s, 3H, 25-H_3), 0.80 (s, 3H, 24-H_3), 0.78 (s, 3H, 23-H_3), 0.74 (d, J = 8.5 Hz, 1H, 5-H) ppm; ^{11}B NMR (160 MHz, $CDCl_3$): δ = 0.99 (t, J = 31.5 Hz) ppm; ^{19}F NMR (470 MHz, $CDCl_3$): δ = −130.07–-132.33 (m) ppm; ^{13}C NMR (126 MHz, $CDCl_3$): δ = 174.1 (C-28), 171.1 (C-31), 170.4 (C-35), 161.9 (C-51), 160.5 (C-55), 154.0 (C-40), 151.0 (C-20), 146.8 (C-49), 145.3 (C-56), 141.7 (C-42), 135.8 (C-36), 134.2 (C-39), 132.6 (C-47), 132.5 (C-43), 131.8 (C-44), 129.8 (C-59), 129.6 (C-48), 129.4 (C-53+C-53′), 129.4 (C-58+C-58′), 129.2 (C-46+C-46′), 129.1 (C-37+C-37′), 128.6 (C-45+C-45′), 128.6 (C-57+C-57′), 127.3 (C-38+C-38′), 122.7 (C-52), 120.1 (C-50), 117.8 (C-41), 116.3 (C-54-H + C-54′), 109.4 (C-29), 81.0 (C-3), 55.5 (C-5), 54.7 (C-17), 52.6 (C-9), 50.7 (C-18), 47.9 (C-34+C-34′), 45.6 (C-19), 42.5 (C-33+C-33′), 41.9 (C-14), 40.7 (C-8), 38.4 (C-1), 37.8 (C-4), 37.1 (C-10), 36.9 (C-13), 36.0 (C-22), 34.3 (C-7), 32.6 (C-16), 31.3 (C-21), 29.8 (C-15), 27.9 (C-24), 25.6 (C-12), 23.7 (C-2), 21.3 (C-32), 21.1 (C-11), 19.6 (C-30), 18.2 (C-6), 16.4 (C-23), 16.2 (C-25), 16.0 (C-26), 14.6 (C-27) ppm; MS (ESI, $CHCl_3$/MeOH, 4:1): m/z = 1006.5 (30%, $[M]^-$); analysis calcd for $C_{69}H_{78}BF_2N_5O_5$ (1106.22): C 74.92, H 7.11, N 6.33; found: C 74.61, H 7.38, N 6.51.

Declaration of competing interest

The authors declare that they have no known competing financial interests or personal relationships that could have appeared to influence the work reported in this paper.

Data availability

Data will be made available on request.

Acknowledgments

We like to thank Mrs. T. Schmidt for measuring the ESI-MS spectra, and Dr. D. Ströhl, Y. Schiller and S. Ludwig for the NMR spectra. Many thanks are also due to Mr. M. Schneider for measuring the optical rotations, the IR and UV/vis spectra and the micro analyses. The cell lines were kindly provided by Dr. Th. Müller (Dept. of Hematology/Oncology, Martin-Luther-Universität Halle-Wittenberg).

Appendix A. Supplementary data

Supplementary data to this article can be found online at https://doi.org/10.1016/j.ejmcr.2022.100099.

References

[1] F. de Jong, J. Pokorny, B. Manshian, B. Daelemans, J. Vandaele, J.B. Startek, S. Soenen, M. Van der Auweraer, W. Dehaen, S. Rocha, G. Silveira-Dorta, Development and characterization of BODIPY-derived tracers for fluorescent labeling of the endoplasmic reticulum, Dyes Pigments 176 (2020), 108200.

[2] E. Antina, N. Bumagina, Y. Marfin, G. Guseva, L. Nikitina, D. Sbytov, F. Telegin, BODIPY conjugates as functional compounds for medical diagnostics and treatment, Molecules 27 (2022).

[3] F. Qi, H. Yuan, Y.C. Chen, Y. Guo, S.R. Zhang, Z.P. Liu, W.J. He, Z.J. Guo, BODIPY-based monofunctional Pt (II) complexes for specific photocytotoxicity against cancer cells, J. Inorg. Biochem. 218 (2021).

[4] H.Z. Yao, S. Chen, Z.Q. Deng, M.K. Tse, Y.D. Matsuda, G.Y. Zhu, BODI-Pt, a green-light-activatable and carboplatin-based platinum(IV) anticancer prodrug with enhanced activation and cytotoxicity, Inorg. Chem. 59 (2020) 11823–11833.

[5] V. Ramu, S. Gautam, P. Kondaiah, A.R. Chakravarty, Diplatinum(II) catecholate of photoactive boron-dipyrromethene for lysosome-targeted photodynamic therapy in red light, Inorg. Chem. 58 (2019) 9067–9075.

[6] V. Ramu, P. Kundu, P. Kondaiah, A.R. Chakravarty, Maloplatin-B, a cisplatin-based BODIPY-tagged mito-specific "Chemo-PDT" agent active in red light, Inorg. Chem. 60 (2021) 6410–6420.

[7] V. Ramu, P. Kundu, A. Upadhyay, P. Kondaiah, A.R. Chakravarty, Lysosome specific platinum(II) catecholates with photoactive BODIPY for imaging and photodynamic therapy in near-IR light, Eur. J. Inorg. Chem. 2021 (2021) 831–839.

[8] M.K. Raza, S. Gautam, A. Garai, K. Mitra, P. Kondaiah, A.R. Chakravarty, Monofunctional BODIPY-appended imidazoplatin for cellular imaging and mitochondria-targeted photocytotoxicity, Inorg. Chem. 56 (2017) 11019–11029.

[9] M.K. Raza, S. Gautam, P. Howlader, A. Bhattacharyya, P. Kondaiah, A.R. Chakravarty, Pyriplatin-boron-dipyrromethene conjugates for imaging and mitochondria-targeted photodynamic therapy, Inorg. Chem. 57 (2018) 14374–14385.

[10] E. Kitteringham, D. Wu, S. Cheung, B. Twamley, D.F. O'Shea, D.M. Griffith, Development of a novel carboplatin like cytoplasmic trackable near infrared fluorophore conjugate via strain-promoted azide alkyne cycloaddition, J. Inorg. Biochem. 182 (2018) 150–157.

[11] J. Zhou, Y.Z. Zhang, G.C. Yu, M.R. Crawley, C.R.P. Fulong, A.E. Friedman, S. Sengupta, J.F. Sun, Q. Li, F.H. Huang, T.R. Cook, Highly emissive self-assembled BODIPY-platinum supramolecular triangles, J. Am. Chem. Soc. 140 (2018) 7730–7736.

[12] U. Bhattacharyya, B. Kumar, A. Garai, A. Bhattacharyya, A. Kumar, S. Banerjee, P. Kondaiah, A.R. Chakravarty, Curcumin "drug" stabilized in oxidovanadium(IV)-BODIPY conjugates for mitochondria-targeted photocytotoxicity, Inorg. Chem. 56 (2017) 12457–12468.

[13] T.T. Sun, W.H. Lin, W. Zhang, Z.G. Xie, Self-Assembly of amphiphilic drug-dye conjugates into nanoparticles for imaging and chemotherapy, Chem. Asian J. 11 (2016) 3174–3177.

[14] C.S. Wijesooriya, J.A. Peterson, P. Shrestha, E.J. Gehrmann, A.H. Winter, E.A. Smith, A photoactivatable BODIPY probe for localization-based super-resolution cellular imaging, Angew. Chem., Int. Ed. 57 (2018) 12685–12689.

[15] T. Zhang, W. Zhang, M. Zheng, Z.G. Xie, Near-infrared BODIPY-paclitaxel conjugates assembling organic nanoparticles for chemotherapy and bioimaging, J. Colloid Interface Sci. 514 (2018) 584–591.

[16] I.W. Badon, J. Lee, T.P. Vales, B.K. Cho, H.J. Kim, Synthesis and photophysical characterization of highly water-soluble PEGylated BODIPY derivatives for cellular imaging, J. Photochem. Photobiol., A 377 (2019) 214–219.

[17] Z. Ruan, Y.Y. Zhao, P. Yuan, L. Liu, Y.C. Wang, L.F. Yan, PEG conjugated BODIPY-Br-2 as macrophotosensitizer for efficient imaging-guided photodynamic therapy, J. Mater. Chem. B 6 (2018) 753–762.

[18] S.T. Wang, J.T. Li, Z. Ye, J.L. Li, A.H. Wang, J. Hu, S. Bai, J. Yin, Self-assembly of photosensitive and chemotherapeutic drugs for combined photodynamic-chemo cancer therapy with real-time tracing property, Colloid. Surface. 574 (2019) 44–51.

[19] Y. Jang, T.I. Kim, H. Kim, Y. Choi, Y. Kim, Photoactivatable BODIPY platform: light-triggered anticancer drug release and fluorescence monitoring, ACS Appl. Bio Mater. 2 (2019) 2567–2572.

[20] A. Sampedro, A. Ramos-Torres, C. Schwoppe, C. Muck-Lichtenfeld, I. Helmers, A. Bort, I. Diaz-Laviada, G. Fernandez, Hierarchical self-assembly of BODIPY dyes as a tool to improve the antitumor activity of capsaicin in prostate cancer, Angew. Chem., Int. Ed. 57 (2018) 17235–17239.

[21] D.N. Tomilin, L.N. Sobenina, K.B. Petrushenko, I.A. Ushakov, B.A. Trofimov, Design of novel meso-CF3-BODIPY dyes with isoxazole substituents, Dyes Pigments 152 (2018) 14–18.

[22] R. Tiwari, P.S. Shinde, S. Sreedharan, A.K. Dey, K.A. Vallis, S.B. Mhaske, S.K. Pramanik, A. Das, Photoactivatable prodrug for simultaneous release of mertansine and CO along with a BODIPY derivative as a luminescent marker in mitochondria: a proof of concept for NIR image-guided cancer therapy, Chem. Sci. 12 (2020) 2667–2673.

[23] Y.H. Li, J. Zeng, Z. Wang, T.Y. Wang, S.Y. Wu, X.Y. Zhu, X. Zhang, B.H. Shan, C.Z. Gao, S.H. Wang, F.A.-O. Wu, Sulfur-Doped Organosilica Nanodots as a Universal Sensor for Ultrafast Live/Dead Cell Discrimination, Biosensors 12 (2022) 1000.

[24] [1], E.M. Nolan, S.J. Lippard, Small-molecule fluorescent sensors for investigating zinc metalloneurochemistry, Acc. Chem. Res. 42 (2009) 193–203.

[25] J. Yao, M. Yang, Y. Duan, Chemistry, biology, and medicine of fluorescent nanomaterials and related systems: new insights into biosensing, bioimaging, genomics, diagnostics, and therapy, Chem. Rev. 114 (2014) 6130–6178.

[26] T. Myochin, K. Hanaoka, T. Komatsu, T. Terai, T. Nagano, Design strategy for a near-infrared fluorescence probe for matrix metalloproteinase utilizing highly cell permeable boron dipyrromethene, J. Am. Chem. Soc. 134 (2012) 13730–13737.

[27] X. Wu, Z. Li, X.-X. Chen, J.S. Fossey, T.D. James, Y.-B. Jiang, Selective sensing of saccharides using simple boronic acids and their aggregates, Chem. Soc. Rev. 42 (2013) 8032–8048.

[28] A.N. Butkevich, G. Lukinavičius, E. D'Este, S.W. Hell, Cell-permeant large Stokes shift dyes for transfection-free multicolor nanoscopy, J. Am. Chem. Soc. 139 (2017) 12378–12381.

[29] D. Kodr, J. Stankova, M. Rumlova, P. Dzubak, J. Rehulka, T. Zimmermann, I. Krizova, S. Gurska, M. Hajduch, P.B. Drasar, M. Jurasek, Betulinic acid decorated with polar groups and blue emitting BODIPY dye: synthesis, cytotoxicity, cell-cycle analysis and anti-HIV profiling, Biomedicines 9 (2021) 1104.

[30] B. Brandes, S. Hoenke, L. Fischer, R. Csuk, Design, synthesis and cytotoxicity of BODIPY FL labelled triterpenoids, Eur. J. Med. Chem. 185 (2020), 111858.

[31] S. Hoenke, I. Serbian, H.P. Deigner, R. Csuk, Mitocanic di- and triterpenoid rhodamine B conjugates, Molecules 25 (2020) 5443.

[32] O. Kraft, M. Kozubek, S. Hoenke, I. Serbian, D. Major, R. Csuk, Cytotoxic triterpenoid-safirinium conjugates target the endoplasmic reticulum, Eur. J. Med. Chem. 209 (2021), 112920.

[33] V.N. Ingle, S.T. Kharche, U.G. Upadhyay, Glucosylation of 4 '-hydroxychalcones using glucosyl donor, Indian J. Chem. B 44 (2005) 801–805.

[34] J. Murtagh, D.O. Frimannsson, D.F. O'Shea, Azide conjugatable and pH responsive near-infrared fluorescent imaging probes, Org. Lett. 11 (2009) 5386–5389.

[35] M. Strobl, T. Rappitsch, S.M. Borisov, T. Mayr, I. Klimant, NIR-emitting aza-BODIPY dyes - new building blocks for broad-range optical pH sensors, Analyst 140 (2015) 7150–7153.

[36] P. Pfeiffer, K. Kollbach, E. Haack, Halochromic compounds of polyketones, Justus Liebigs Ann. Chem. 460 (1928) 138–156.

[37] M. Farfan-Paredes, O. Gonzalez-Antonio, D.E. Tahuilan-Anguiano, J. Peon, A. Ariza, P.G. Lacroix, R. Santillan, N. Farfan, Physicochemical and computational insight of F-19 NMR and emission properties of meso-(o-aryl)-BODIPYs, New J. Chem. 44 (2020) 19459–19471.

[38] S. Grigoropoulou, D. Manou, A.I. Antoniou, A. Tsirogianni, C. Siciliano, A.D. Theocharis, C.M. Athanassopoulos, Synthesis and antiproliferative activity of novel dehydroabietic acid-chalcone hybrids, Molecules 27 (2022) 3623.

[39] H.H.H. Mohammed, A.A. Abd El-Hafeez, K. Ebeid, A.I. Mekkawy, M.A.S. Abourehab, E.I. Wafa, S.O. Alhaj-Suliman, A.K. Salem, P. Ghosh, G.E.A. Abuo-Rahma, A.M. Hayallah, S.H. Abbas, New 1,2,3-triazole linked ciprofloxacin-chalcones induce DNA damage by inhibiting human topoisomerase I& II and tubulin polymerization, J. Enzym. Inhib. Med. Chem. 37 (2022) 1346–1363.

[40] N.A. Rehuman, J.M. Oh, M.A. Abdelgawad, E.A.M. Beshr, M.A.S. Abourehab, N. Gambacorta, O. Nicolotti, R.K. Jat, H. Kim, B. Mathew, Development of halogenated-chalcones bearing with dimethoxy phenyl head as monoamine oxidase-B inhibitors, Pharmaceuticals 15 (2022) 1152.

[41] E.A. Veliz, A. Kaplina, S.D. Hettiarachchi, A.L. Yoham, C. Matta, S. Safar, M. Sankaran, E.L. Abadi, E.K. Cilingir, F.A. Vallejo, W.M. Walters, S. Vanni, R.M. Leblanc, R.M. Graham, Chalcones as anti-glioblastoma stem cell agent alone or as nanoparticle formulation using carbon dots as nanocarrier, Pharmaceutics 14 (2022) 1465.

[42] S. Li, R.A.-O. Wu, L. Wang, H.C. Dina Kuo, D. Sargsyan, X. Zheng, Y. Wang, X. Su, A.A.-O. Kong, Triterpenoid ursolic acid drives metabolic rewiring and epigenetic reprogramming in treatment/prevention of human prostate cancer, Mol. Carcinogen 61 (2022) 111–121.

[43] D.M. Gurfinkel, S. Chow, R. Hurren, M. Gronda, C. Henderson, C. Berube, D.W. Hedley, A.D. Schimmer, Disruption of the endoplasmic reticulum and increases in cytoplasmic calcium are early events in cell death induced by the natural triterpenoid Asiatic acid, Apoptosis 11 (2006) 1463–1471.

[44] D. Luo, N. Fan, X. Zhang, F.Y. Ngo, J. Zhao, W. Zhao, M. Huang, D. Li, Y. Wang, J. Rong, Covalent inhibition of endoplasmic reticulum chaperone GRP78 disconnects the transduction of ER stress signals to inflammation and lipid accumulation in diet-induced obese mice, Elife 11 (2022), e72182.